Sensitization of Lanthanide Luminescence in Heterotrinuclear $PtLn_2$ (Ln = Eu, Nd, Yb) Complexes with Terpyridyl-Functionalized Alkynyl by Energy Transfer from a Platinum(II) Alkynyl Chromophore

Xiu-Ling Li,[†,‡] Feng-Rong Dai,[†] Li-Yi Zhang,[†] Yue-Mei Zhu,[†] Qi Peng,[†] and Zhong-Ning Chen*[,†]

State Key Laboratory of Structural Chemistry, Fujian Institute of Research on the Structure of Matter, Chinese Academy of Sciences, Fuzhou, Fujian 350002, People's Republic of China, and the School of Chemistry and Chemical Engineering, Xuzhou Normal University, Xuzhou, Jiangsu 221116, People's Republic of China

Received February 9, 2007

The preparation and characterization of the mononuclear complexes *cis*-Pt(dppe)(C≡CPhtpy)$_2$ (**1**) and *cis*-Pt(dppp)(C≡CPhtpy)$_2$ (**5**) (dppe = 1,2-bis(diphenylphosphino)ethane, dppp = 1,3-bis(diphenylphosphino)propane, HC≡CPhtpy = 4′-(4-ethynylphenyl)-2,2′:6′,2″-terpyridine) and the corresponding $PtLn_2$ (Ln = Eu, Nd, Yb) heterotrinuclear complexes by incorporating the precursor **1** or **5** with Ln(hfac)$_3$-(H$_2$O)$_2$ are described. **1** and **5** exhibit intense, long-lived room-temperature phosphorescence, originating probably from an admixture of ^{3}ILCT ($\pi \rightarrow \pi^*$(C≡Cphtpy)) and ^{3}MLCT (d(Pt) $\rightarrow \pi^*$(C≡CPhtpy)) triplet states, which qualifies them as favorable energy donors to facilitate Pt → Ln energy transfer in the corresponding $PtLn_2$ heterotrinuclear complexes. As anticipated, sensitized lanthanide luminescence in $PtLn_2$ heterotrinuclear complexes is attained through efficient energy transfer from Pt^{II} alkynyl chromophore based ^{3}MLCT and ^{3}ILCT triplet states.

Introduction

Lanthanide(III) luminescence, especially near-infrared (near-IR) emission, has received much attention, due to its extensive applications in light-emitting diodes, optical communication, light amplifiers, biological assays, etc.[1] Because of the weak absorption of forbidden f−f transitions, luminescence from Ln^{III} ions is usually sensitized by antenna chromophores through efficient energy transfer.[1a] Traditionally, sensitization of lanthanide luminescence is achieved by π-conjugated organic aromatic chromophores that are directly coordinated to the lanthanide centers and strongly absorb UV light.[1a] Recently, a new approach has been developed using transition-metal-containing antenna chromophores as lanthanide sensitizers.[1c−e,2] The d-block-metal-containing chromophores afford a series of advantages, including (i) low-energy absorption in the visible region arising from red-shifted ILCT (intraligand charge transfer) or MLCT (metal-to-ligand charge transfer) transitions, causing a better energy match between d-block donors and Ln^{III} acceptors and thus less waste in energy,[1a,c,e,2] (ii) relatively high triplet quantum yields resulting from the rapid intersystem crossing induced by the heavy-metal effect,[3] (iii) relatively long-lived triplet excited states that facilitate energy transfer to the adjacent lanthanide centers,[1a,c,e,2] and (iv) facile detection of both quenching of the d-block chromophores and the sensitized emission from the lanthanide centers.

In recent years, considerable attention has been paid to carbon-rich Pt−alkynyl complexes, due to their rigid structures as well as rich spectroscopic and luminescent properties associated with diverse charge-transfer transitions.[4] Particularly, Pt−alkynyl−phosphine complexes frequently display attractive room-temperature phosphorescence associated with strong spin-orbital coupling due to the heavy-atom effect of the platinum-(II) ion.[5] It is anticipated that these Pt−alkynyl−phosphine moieties may serve as favorable d-block chromophore donors for sensitization of lanthanide luminescence if the alkynyl ligands are functionalized appropriately.[1c,2a] A series of Pt_2Ln_2

* To whom correspondence should be addressed. E-mail: czn@fjirsm.ac.cn.
† Fujian Institute of Research on the Structure of Matter.
‡ Xuzhou Normal University.

(1) (a) Bünzli, J.-C. G.; Piguet, C. *Chem. Soc. Rev.* **2005**, *34*, 1048. (b) Zheng, Z. *Chem. Commun.* **2001**, 2521. (c) Xu, H. B.; Shi, L. X.; Ma, E.; Zhang, L. Y.; Wei, Q. H.; Chen, Z. N. *Chem. Commun.* **2006**, 1601. (d) Zang, F. X.; Hong, Z. R.; Li, W. L.; Li, M. T.; Sun, X. Y. *Appl. Phys. Lett.* **2004**, *84*, 2679. (e) Guo, D.; Duan, C. Y.; Lu, F.; Hasegawa, Y.; Meng, Q. J.; Yanagida, S. *Chem. Commun.* **2004**, 1486.

(2) (a) Ronson, T. K.; Lazarides, T.; Adams, H.; Pope, S. J. A.; Sykes, D.; Faulkner, S.; Coles, S. J.; Hursthouse, M. B.; Clegg, W.; Harrington, R. W.; Ward, M. D. *Chem. Eur. J.* **2006**, *12*, 9299. (b) Beer, P. D.; Szemes, F.; Passaniti, P.; Maestri, M. *Inorg. Chem.* **2004**, *43*, 3965. (c) Klink, S. I.; Keizer, H.; van Veggel, F. C. J. M. *Angew. Chem., Int. Ed.* **2000**, *39*, 4319. (d) Shavaleev, N. M.; Moorcraft, L. P.; Pope, S. J. A.; Bell, Z. R.; Faulkner, S.; Ward, M. D. *Chem. Eur. J.* **2003**, *9*, 5283. (e) Shavaleev, N. M.; Moorcraft, L. P.; Pope, S. J. A.; Bell, Z. R.; Faulkner, S.; Ward, M. D. *Chem. Commun.* **2003**, 1134. (f) Shavaleev, N. M.; Accorsi, G.; Virgili, D.; Bell, Z. R.; Lazarides, T.; Calogero, G.; Armaroli, N.; Ward, M. D. *Inorg. Chem.* **2005**, *44*, 61.

(3) (a) Haskins-Glusac, K.; Ghiviriga, I.; Abbound, K. A.; Schanze, K. S. *J. Phys. Chem. B* **2004**, *108*, 4969. (b) Baldo, M. A.; O'Brien, D. F.; You, Y.; Shoustikov, A.; Sibley, S.; Thompson, M. E.; Forrest, S. R. *Nature* **1998**, *395*, 151. (c) Adachi, C.; Baldo, M. A.; Thompson, M. E.; Forrest, S. R. *J. Appl. Phys.* **2001**, *90*, 5048.

(4) Yam, V. W. W.; Wong, K. M. C.; Zhu, N. *Angew. Chem., Int. Ed.* **2003**, *42*, 1400.

(5) (a) Saha, R.; Qaium, Md. A.; Debnath, D.; Younus, M.; Chawdhury, N.; Sultana, N.; Kociok-Köhn, G.; Ooi, L. L.; Raithby, P. R.; Kijima, M. *Dalton Trans.* **2005**, 2760. (b) Tao, C. H.; Zhu, N.; Yam, V. W. W. *Chem. Eur. J.* **2005**, *11*, 1647. (c) Yam, V. W. W.; Chan, L. P.; Lai, T. F. *Organometallics* **1993**, *12*, 2197. (d) Yam, V. W. W.; Yeung, P. K. Y.; Chan, L. P.; Kwok, W. M.; Phillips, D. L.; Yu, K. L.; Wong, R. W. K.; Yan, H.; Meng, Q. J. *Organometallics* **1998**, *17*, 2590. (e) Silverman, E. E.; Cardolaccia, T.; Zhao, X. M.; Kim, K. Y.; Haskins-Glusac, K.; Schanze, K. S. *Coord. Chem. Rev.* **2005**, *249*, 1491.

10.1021/om070130h CCC: $37.00
Publication on Web 07/27/2007

or Pt_2Ln_4 complexes have been prepared using diimine-functionalized alkynyl ligands, in which the reaction of $PtCl_2$(dppm-P, P′) (dppm = bis(diphenylphosphino)methane) with 5-ethynyl-2,2′-bipyridine or 5-ethynyl-1,10-phenanthroline gave the face-to-face diplatinum clusters $Pt_2(\mu\text{-dppm})_2(C{\equiv}CR)_4$ (R = 2,2′-bpy, 1,10-phen), subsequent incorporation with $Ln(hfac)_3$ (Hhfac = hexafluoroacetylacetone) through 2,2′-bpy or 1,10-phen chelation affording the desired $Pt^{II}{-}Ln^{III}$ arrays.[1c] As anticipated, sensitized lanthanide luminescence by the d(Pt) → π^*(C≡CR) MLCT excited state is attained through efficient energy transfer from the Pt^{II} alkynyl antenna chromophores to the lanthanide centers.[1c]

As a conjugated polyaromatic bridging ligand with both "soft" acetylide donors for transition-metal centers and "hard" terpyridyl donors for lanthanide centers, it is anticipated that 4′-(4-ethynylphenyl)-2,2′:6′,2″-terpyridine (HC≡CPhtpy) is another excellent candidate for the construction of d−f heterometallic arrays containing d-block antenna chromophores as energy donors and lanthanide centers as energy acceptors, allowing sensitization of the lanthanide emission through energy transfer from the d-block chromophores. By this consideration, the mononuclear precursors *cis*-Pt(dppe)(C≡CPhtpy)$_2$ (**1**) and *cis*-Pt(dppp)(C≡CPhtpy)$_2$ (**5**) (dppe = 1,2-bis(diphenylphosphino)-ethane, dppp = 1,3-bis(diphenylphosphino)propane) were prepared by reaction of HC≡CPhtpy with *cis*-Pt(dppe)Cl_2 or *cis*-Pt(dppp)Cl_2. The two mononuclear Pt^{II} complexes exhibit intense, long-lived, room-temperature phosphorescence originating from an admixture of ^{3}ILCT ($\pi \rightarrow \pi^*$(C≡Cphtpy)) and ^{3}MLCT (d(Pt) → π^*(C≡CPhtpy)) transitions, which qualifies them as excellent energy donors to facilitate Pt → Ln energy transfer in $PtLn_2$ heterotrinuclear arrays originating from incorporation of **1** or **5** with $Ln(hafc)_3(H_2O)_2$. As expected, sensitization of luminescence from lanthanide centers is achieved by excitation of a Pt^{II} alkynyl based MLCT transition, suggesting that $Pt^{II} \rightarrow Ln^{III}$ energy transfer indeed occurs from the Pt-based antenna chromophores. In this paper, we describe the syntheses, characterization, and photophysical properties of mononuclear platinum−alkynyl−diphosphine precursors of HC≡CPhtpy and their corresponding heterotrinuclear $PtLn_2$ (Ln = Eu, Nd, Yb) adducts by incorporation with $Ln(hfac)_3$ units.

Experimental Section

Materials and Reagents. All reactions were carried out under a dry argon atmosphere by using Schlenk techniques at ambient temperature and a vacuum-line system, unless otherwise specified. The solvents were dried, distilled, and degassed prior to use, except those for spectroscopic measurements, which were of spectroscopic grade. The reagents dppe and dppp were purchased from Acros. HC≡CPhtpy, *cis*-Pt(dppe)Cl_2, and *cis*-Pt(dppp)Cl_2 were prepared as reported in the literature.[6−8]

Pt(dppe)(C≡CPhtpy)$_2$ (1). Pt(dppe)Cl_2 (158 mg, 0.24 mmol) and CuI (5.8 mg, 0.030 mmol) suspended in acetonitrile (2 mL) and diisopropylamine (3 mL) were added successively to a THF (80 mL) solution of HC≡CPhtpy (173 mg, 0.52 mmol). The mixture was stirred for 7 days at room temperature, and then any volatile components were removed under reduced pressure. The resulting solid was successively washed three times with water, ethanol, and dichloromethane, respectively. The product was dried in vacuo, affording a greenish yellow solid. Yield: 90%. Anal. Calcd for $C_{72}H_{52}N_6P_2Pt{\cdot}CH_2Cl_2$: C, 65.28; H, 4.05; N, 6.26. Found: C, 65.25; H, 4.09; N, 6.23. ES-MS (*m/z*): 1259.9 [(M + H$^+$)]. IR (KBr, cm^{-1}): ν 2107 (s, C≡C). The poor solubility of **1** in common organic solvents hindered NMR spectral measurements.

Table 1. Crystallographic Data for 1·3CH_2Cl_2, 6·$^1/_2CH_2Cl_2{\cdot}^5/_2H_2O$, and 8·$^1/_2CH_2Cl_2{\cdot}^1/_2H_2O$

	1·3CH_2Cl_2	**6**·$^1/_2CH_2Cl_2{\cdot}^5/_2H_2O$	**8**·$^1/_2CH_2Cl_2{\cdot}^1/_2H_2O$
empirical formula	$C_{75}H_{58}Cl_6N_6P_2Pt$	$C_{103.50}H_{66}ClEu_2F_{36}N_6O_{14.5}P_2Pt$	$C_{103}H_{60}F_{36}N_6O_{12}P_2PtYb_2$
formula wt	1512.99	2906.02	2912.15
temp, K	293(2)	293(2)	293(2)
space group	*C*2/*c*	$P\bar{1}$	$P\bar{1}$
a, Å	17.395(3)	12.600(3)	12.714(7)
b, Å	20.404(4)	22.070(5)	22.082(12)
c, Å	20.415(4)	24.810(6)	25.136(12)
α, deg		78.220(8)	78.376(16)
β, deg	109.659(3)	77.680(6)	78.315(18)
γ, deg		85.220(8)	84.879(16)
V, Å^3	6823(2)	6593(3)	6760(6)
Z	4	2	2
ρ_{calcd}, g cm^{-3}	1.473	1.464	1.431
μ, mm^{-1}	2.386	2.147	2.547
radiation (λ), Å	0.710 73	0.710 73	0.710 73
R1[a]	0.0363	0.0711	0.0999
wR2[b]	0.0958	0.1847	0.2637
GOF	1.058	1.100	1.038

[a] $R1 = \sum|F_o - F_c|/\sum F_o$. [b] $wR2 = \sum[w(F_o^2 - F_c^2)^2]/\sum[w(F_o^2)]^{1/2}$.

{Pt(dppe)(C≡CPhtpy)$_2$}{Ln(hfac)$_3$}$_2$ (Ln = Eu (2), Nd (3), Yb (4)). These compounds were prepared by reaction of **1** with 4 equiv of $Ln(hfac)_3(H_2O)_2$ in dichloromethane with stirring for 2 h at room temperature. After filtration, the solutions were concentrated to precipitate the greenish yellow or orange products by addition of *n*-hexane. Layering *n*-hexane onto the concentrated dichloromethane solutions gave the products as rodlike crystals.

2: yield 82%. Anal. Calcd for $C_{102}H_{58}Eu_2F_{36}N_6O_{12}P_2Pt$: C, 43.68; H, 2.08; N, 3.00. Found: C, 43.55; H, 2.10; N, 2.97. IR (KBr, cm^{-1}): ν 2112 (m, C≡C), 1655 (vs, C═O).

3: yield 82%. Anal. Calcd for $C_{102}H_{58}F_{36}N_6Nd_2O_{12}P_2Pt$: C, 43.93; H, 2.10; N, 3.01. Found: C, 43.83; H, 2.13; N, 2.98. IR (KBr, cm^{-1}): ν 2111 (m, C≡C), 1652 (vs, C═O).

4: yield 90%. Anal. Calcd for $C_{102}H_{58}F_{36}N_6O_{12}P_2PtYb_2{\cdot}2CH_2Cl_2$: C, 41.41; H, 2.07; N, 2.79. Found: C, 41.79; H, 2.09; N, 2.78. IR (KBr, cm^{-1}): ν 2114 (m, C≡C), 1658(vs, C═O).

Pt(dppp)(C≡CPhtpy)$_2$ (5). This complex was prepared by the same procedure as for **1**, except for the use of Pt(dppp)Cl_2 instead of Pt(dppe)Cl_2. The product was purified by chromatography on a silica gel column using dichloromethane−methanol (50/1 v/v) as an eluent and collected as a yellow band. Subsequent recrystallization from dichloromethane−diethyl ether gave **2** as a yellow solid. Yield: 71%. Anal. Calcd for $C_{73}H_{54}N_6P_2Pt$: C, 68.91; H, 4.28; N, 6.61. Found: C, 68.60; H, 4.30; N, 6.57. ES-MS (*m/z*): 1273.1 [M + H$^+$], 939.1 [M − C≡CPhtpy]$^+$. IR (KBr, cm^{-1}): ν 2117 (s, C≡C). ^{1}H NMR (500 MHz, $CDCl_3$, ppm): δ 8.71−8.64 (m, 12H, tpy); 7.84−7.71 (m, 12H, C_6H_5); 7.61 (d, 4H, J_{H-H} = 7.5 Hz, C≡CC_6H_4); 7.43−7.39 (m, 8H, tpy); 7.34−7.33 (m, 8H, C_6H_5); 6.95 (d, 4H, J_{H-H} = 7.5 Hz, C≡CC_6H_4); 2.55 (s, broad, 4H, $PCH_2CH_2CH_2P$); 2.09 (s, broad, 2H, $PCH_2CH_2CH_2P$). ^{31}P NMR (202.3 MHz, $CDCl_3$, ppm): −5.5 (s, J_{Pt-P} = 1112 Hz).

{Pt(dppp)(C≡CPhtpy)$_2$}{Ln(hfac)$_3$}$_2$ (Ln = Eu (6), Nd (7), Yb (8)). The synthetic procedures for **6**−**8** are the same as those for **2**−**4**, except **5** was used in place of **1**. Layering *n*-hexane onto the concentrated dichloromethane solutions gave the complexes as orange or orange-red crystals.

6: yield 51%. Anal. Calcd for $C_{103}H_{60}Eu_2F_{36}N_6O_{12}P_2Pt$: C, 43.89; H, 2.15; N, 2.98. Found: C, 43.60; H, 2.18; N, 2.95. IR (KBr, cm^{-1}): ν 2117 (m, C≡C), 1655 (vs, C═O).

7: yield 45%. Anal. Calcd for $C_{103}H_{60}F_{36}N_6Nd_2O_{12}P_2Pt$: C, 44.13; H, 2.16; N, 3.00. Found: C, 43.90; H, 2.21; N, 2.95. IR (KBr, cm^{-1}): ν 2116 (m, C≡C), 1653 (vs, C═O).

(6) Grosshenny, V.; Romero, F. M.; Ziessel, R. *J. Org. Chem.* **1997**, *62*, 1491.
(7) Yasufuka, K.; Noda, H.; Y.; Yamazaki, H.; Martinengo, S. *Inorg. Synth.* **1989**, *26*, 369.
(8) Slack, D. A.; Baird, M. C. *Inorg. Chim. Acta* **1977**, *24*, 277.

Scheme 1. Synthetic Routes to 1−8

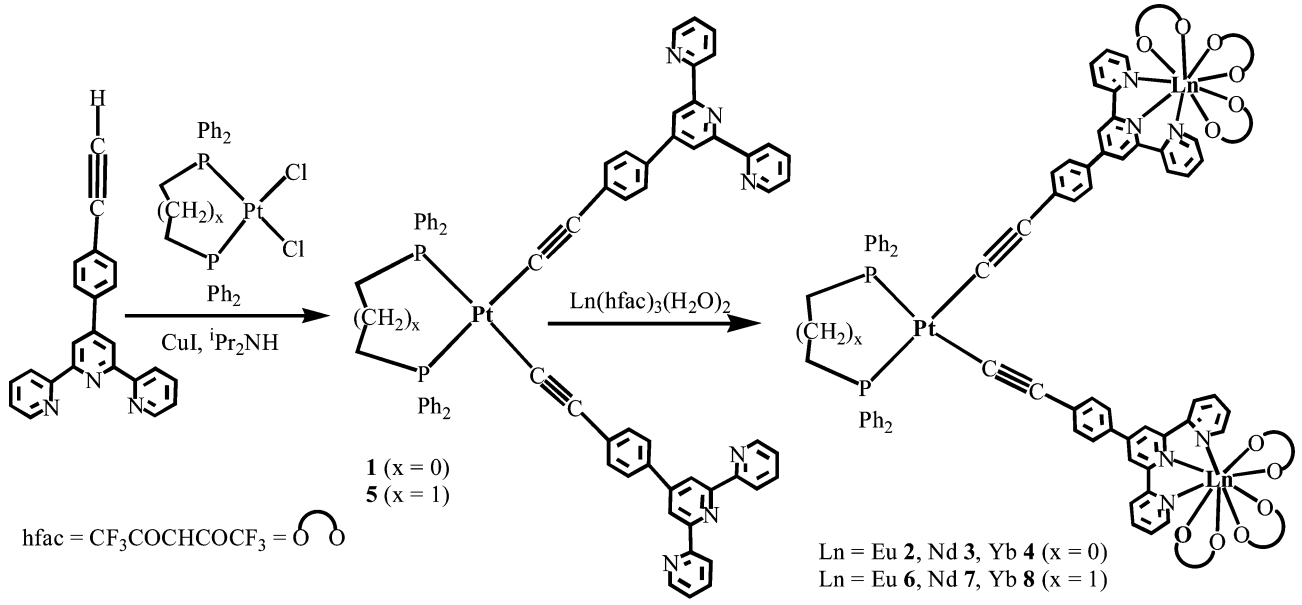

8: yield 47%. Anal. Calcd for $C_{103}H_{60}F_{36}N_6O_{12}P_2PtYb_2$: C, 43.25; H, 2.11; N, 2.94. Found: C, 43.15; H, 2.14; N, 2.93. IR (KBr, cm^{-1}): ν 2118 (m, C≡C), 1656 (vs, C═O).

Crystal Structure Determinations. Crystals suitable for X-ray diffraction studies were obtained by layering *n*-hexane onto the dichloromethane solutions. Single crystals sealed in capillaries with their mother liquors were measured on a Rigaku MERCURY CCD diffractometer by ω-scan techniques at room temperature using graphite-monochromated Mo Kα radiation (λ = 0.710 73 Å). The CrystalClear software package was used for data reduction and empirical absorption correction. The structures were solved by direct methods.[9] The heavy atoms were located from an E map, and the other non-hydrogen atoms were located according to the successive least-squares Fourier cycles. Most of the non-hydrogen atoms were refined anisotropically, except for some disordered atoms, whereas the hydrogen atoms were generated geometrically with isotropic thermal parameters. The structures were refined on F^2 by full-matrix least-squares methods using the SHELXTL-97 program package.[9]

The crystals of **6**·$^1/_2CH_2Cl_2$·$^5/_2H_2O$ and **8**·$^1/_2CH_2Cl_2$·$^1/_2H_2O$ diffracted poorly; thus, the refined results are not perfect. For some disordered $-CF_3$ groups, restrained refinements were carried out by fixing the C−F distances at 1.31 Å with the occupancy factors of F and F′ atoms being 0.50, respectively. The crystallographic data of **1**·$3CH_2Cl_2$, **6**·$^1/_2CH_2Cl_2$·$^5/_2H_2O$, and **8**·$^1/_2CH_2Cl_2$·$^1/_2H_2O$ are summarized in Table 1.

Physical Measurements. UV−vis absorption spectra were obtained using a Perkin-Elmer Lambda 25 UV−vis spectrometer. Infrared (IR) spectra were recorded on a Magna750 FT-IR spectrophotometer with KBr pellets. Elemental analyses (C, H, N) were carried out on a Perkin-Elmer Model 240C elemental analyzer. Electrospray mass spectra (ES-MS) were performed on a Finnigan LCQ mass spectrometer using dichloromethane−methanol mixtures as mobile phases. The ^1H and ^{31}P NMR spectra were measured on a Varian UNITY-500 spectrometer with $SiMe_4$ as an internal reference and 85% H_3PO_4 as an external standard, respectively. Emission and excitation spectra in the UV−vis region and luminescence titration processes were recorded on a Perkin-Elmer LS 55 luminescence spectrometer with an R928 red-sensitive photomultiplier without correction. The steady-state near-infrared (near-IR) emission spectra were measured on an Edinburgh FLS920 fluorescence spectrometer equipped with a Hamamatsu R5509-72 supercooled photomultiplier tube at 193 K and a TM300 emission monochromator with a near-IR grating blazed at 1000 nm. Near-IR emission spectra were corrected via a calibration curve supplied with the instrument. Emission lifetimes were obtained by using an Edinburgh Xe900 450 W pulse xenon lamp as the excitation light source. The emission quantum yields of compounds **1**, **2**, **5**, and **6** were measured in degassed dichloromethane solutions at 298 K, estimated relative to $[Ru(bpy)_3](PF_6)_2$ in acetonitrile as the standard (Φ_{em} = 0.062), and calculated by $\Phi_s = \Phi_r(B_r/B_s)(n_s/n_r)^2(D_s/D_r)$, where the subscripts r and s denote the reference standard and the sample solution, respectively, n is the refractive index of the solvents; D is the integrated intensity, and Φ is the luminescence quantum yield. The quantity B is calculated by $B = 1 - 10^{-AL}$, where A is the absorbance at the excitation wavelength and L is the optical path length.[10]

Results and Discussion

Syntheses and Characterization. As shown in Scheme 1, **1** and **5** were prepared by reaction of $Pt(dppe)Cl_2$ or $Pt(dppp)Cl_2$ with 2.2 equiv of HC≡CPhtpy in dichloromethane solution, catalyzed by CuI in the presence of $^iPr_2NH$.[5a,11,12] **1** was sparsely soluble in common solvents and could be readily purified by washing with water, ethanol, and dichloromethane to remove the small impurities. **5** was purified by silica gel column chromatography and collected as a yellow band. Both compounds were characterized by elemental analyses, ESI-MS spectrometry, and IR and UV−vis absorption spectra, and 5 was characterized by ^1H and ^{31}P NMR spectroscopy. In the ^{31}P NMR spectrum (Figure S1, Supporting Information) of **5**, typical P satellite peaks caused by the Pt−P coupling occur at −5.5 ppm with J_{Pt-P} = 1112 Hz, coinciding with those reported in the literature.[5a,13] Nevertheless, **1** was not sufficiently soluble in common solvents for NMR spectral measurement.

(9) Sheldrick, G. M. SHELXS-97 and SHELXL-97; University of Göttingen, Göttingen, Germany, 1997.

(10) (a) Demas, J. N.; Crosby, G. A. *J. Phys. Chem.* **1971**, *75*, 991. (b) Chan, S. C.; Chan, M. C. W.; Wang, Y.; Che, C. M.; Cheung, K. K.; Zhu, N. *Chem. Eur. J.* **2001**, *7*, 4180.

(11) (a) Hissler, M.; Ziessel, R. *J. Chem. Soc., Dalton Trans.* **1995**, 893. (b) Harriman, A.; Hissler, M.; Ziessel, R.; De Cian, A.; Fisher, J. *J. Chem. Soc., Dalton Trans.* **1995**, 4067.

(12) Janka, M.; Anderson, G. K.; Rath, N. P. *Organometallics* **2004**, *23*, 4382.

(13) Whiteford, J. A.; Lu, C. V.; Stang, P. J. *J. Am. Chem. Soc.* **1997**, *119*, 2524.

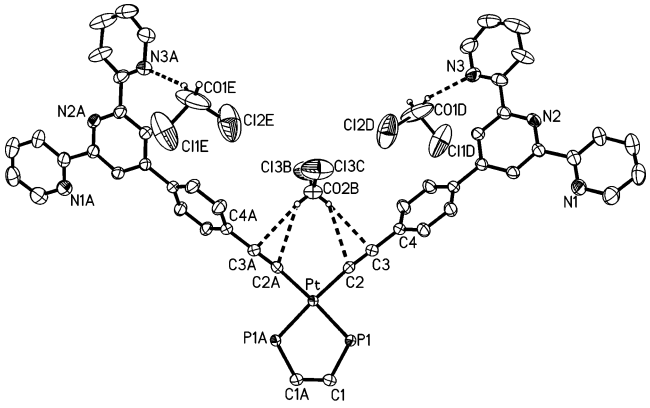

Figure 1. ORTEP drawing of **1**·3CH_2Cl_2 with the atom-labeling scheme, showing 30% thermal ellipsoids. The phenyl rings of dppe are omitted for clarity.

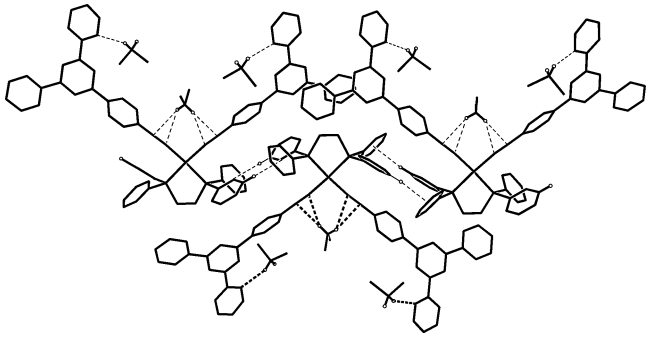

Figure 2. Chain structure of **1**·3CH_2Cl_2 resulting from the C−H···π aromatic interaction between the phenyl rings of dppe. Hydrogen atoms are omitted for clarity, except for H32A and those of CH_2Cl_2.

Reactions of **1** and **5** with an excess of $Ln(hfac)_3(H_2O)_2$ in dichloromethane solution induced isolation of the $PtLn_2$ heterotrinuclear adducts **2**−**4** and **6**−**8**, respectively. While $Ln(hfac)_3(H_2O)_2$ and **1** are sparsely soluble in dichloromethane, the solubility improves significantly upon formation of the $PtLn_2$ heterotrinuclear arrays. The structures of **1**, **6**, and **8** were determined by single-crystal X-ray diffraction. In the IR spectra of **1**−**8**, the C≡C stretching frequencies in the range 2107−2118 cm^{-1} are typical for Pt^{II} species with terminally coordinated alkynyls.[5b,12,14] The $PtLn_2$ complexes display typical C=O stretching frequencies at ca. 1652−1658 cm^{-1}, confirming the incorporation of the $Ln(hfac)_3$ unit into **1** or **5**.

Crystal Structures. The molecular structures of **1**·3CH_2Cl_2, **6**·$^1/_2CH_2Cl_2$·$^5/_2H_2O$, and **8**·$^1/_2CH_2Cl_2$·$^1/_2H_2O$ are shown in Figures 1 and 3 and Figure S2 (Supporting Information), respectively. Selected bond lengths and bond angles are presented in Table 2.

1·3CH_2Cl_2 crystallizes in the monoclinic system with the space group *C*2/*c*. The Pt^{II} center adopts an essentially square-planar geometry with slight distortion due to the coordination constraints imposed by the dppe ligand (C2−Pt−P1 = 89.46(13)°, P1−Pt−P1a = 86.69(6)°, C2−Pt−C2a = 94.4(3)°). The sum of the angles around the Pt^{II} center is 360°. The Pt−C≡C−C arrays show some deviation from linearity with Pt−C2−C3 = 173.7(4)° and C2−C3−C4 = 178.5(6)°. The Pt−P and Pt−C distances are 2.259(1) and 2.031(5) Å, respectively, in good agreement with the lengths in analogous Pt−acetylide systems.[3a,13,15] The C2−C3 distance (1.181(7) Å) is slightly longer than that of the free C≡C bond (1.143(8) Å) in the tridentate chelating Cu^I complex of HC≡CPhtpy.[16] The phenyl ring in C≡CPhtpy forms a dihedral angle of 60.4° with the Pt^{II} coordination plane defined by C_2P_2 donors. The C≡CPhtpy group shows great flexibility, with its phenyl ring making an angle of 32.8° with the middle pyridyl ring of the terpyridyl moiety. The middle pyridyl ring forms dihedral angles of 7.1 and 15.9° with the pyridyl rings containing the N1 and N3 atoms, respectively. The chelating dppe ligand adopts a gauche conformation with a P−CH_2−CH_2−P torsion angle of 13.5°. The shortest distance between adjacent Pt^{II} atoms in the crystal is 10.99 Å, indicating the absence of Pt−Pt contacts in the crystal lattice. As shown in Figure 1, one solvated dichloromethane molecule is located between two C≡Cphtpy ligands in **1**·3CH_2Cl_2. The C2···H04B and C3···H04B (B: 0.5 + *x*, −0.5 + *y*, +*z*) distances are 2.809 and 2.676 Å, respectively, which are slightly shorter than the sum of van der Waals radii for H and C (2.9 Å)[17] and comparable to the C−H···π (C≡C) distances in $(Ar_3P)AuC{\equiv}CAu(PAr_3)\cdot(CHCl_3)_n$ ($d_{H\cdots C}$ = 2.45−2.70 Å; *n* = 2, Ar_3 = $NpPh_2$; *n* = 6, Ar_3 = Np_2Ph, Np =

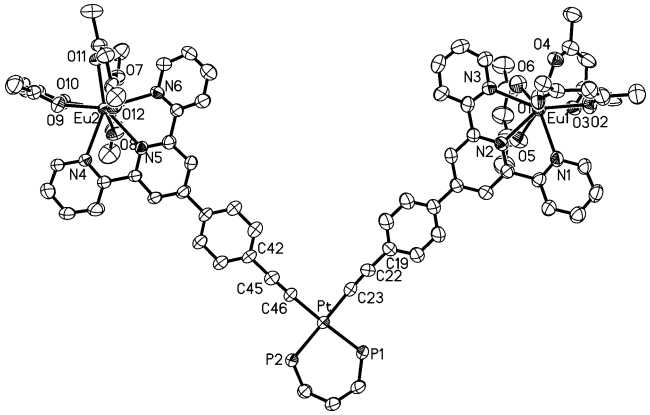

Figure 3. ORTEP view of **6** with the atom-labeling scheme, showing 30% thermal ellipsoids. The phenyl rings of dppp and F atoms in the $-CF_3$ groups are omitted for clarity.

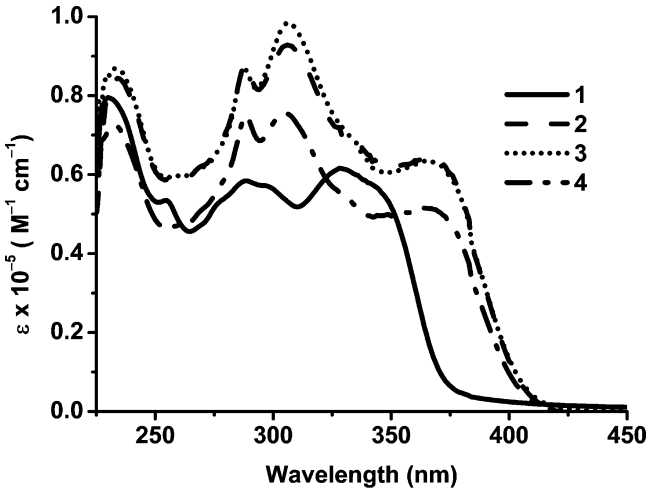

Figure 4. UV−vis absorption spectra of **1**−**4** in dichloromethane solutions.

(14) (a) Bruce, M. I.; Costuas, K.; Halet, J. F.; Hall, B. C.; Low, P. J.; Nicholson, B. K.; Skelton, B. W.; White, A. H. *Dalton Trans.* **2002**, 383. (b) Johnson, C. A., II; Haley, M. M. *Organometallics* **2005**, *24*, 1161. (c) Lam, S. C. F.; Yam, V. W. W.; Wong, K. M. C.; Cheng, E. C. C.; Zhu, N. *Organometallics* **2005**, *24*, 4298.

(15) Baraban, J. M.; McGinnety, J. A. *Inorg. Chem.* **1974**, *13*, 2864. (b) Mayor, M.; von Hänisch, C.; Weber, H. B.; Reichert, J.; Beckmann, D. *Angew. Chem., Int. Ed.* **2002**, *41*, 1183.

(16) Constable, E. C.; Housecroft, C. E.; Neuburger, M.; Schaffner, S.; Shardlow, E. J. *Inorg. Chem. Commun.* **2005**, *8*, 743.

(17) Bondi, A. *J. Phys. Chem.* **1964**, *68*, 441.

Table 2. Selected Bond Distances (Å) and Angles (deg) for 1, $6\cdot{}^1/_2CH_2Cl_2\cdot{}^5/_2H_2O$, and $8\cdot{}^1/_2CH_2Cl_2\cdot{}^1/_2H_2O$

$1\cdot 3CH_2Cl_2$		$6\cdot{}^1/_2CH_2Cl_2\cdot{}^5/_2H_2O$		$8\cdot{}^1/_2CH_2Cl_2\cdot{}^1/_2H_2O$	
Pt−P1	2.259(1)	Pt−C23	2.014(10)	Pt−C23	2.025(18)
Pt−C2	2.031(5)	Pt−C46	2.010(9)	Pt−C46	2.03(2)
C2−C3	1.181(7)	Pt−P1	2.293(2)	Pt−P1	2.321(5)
C3−C4	1.440(7)	Pt−P2	2.293(2)	Pt−P2	2.326(5)
C1−P1	1.843(6)	Eu1−O1	2.440(6)	Yb1−O1	2.434(13)
C7−C17	1.486(6)	Eu1−O2	2.377(6)	Yb1−O2	2.360(12)
		Eu1−O3	2.413(6)	Yb1−O3	2.444(13)
		Eu1−O4	2.471(6)	Yb1−O4	2.345(12)
		Eu1−O5	2.406(6)	Yb1−O5	2.432(14)
		Eu1−O6	2.478(6)	Yb1−O6	2.330(15)
		Eu1−N4	2.604(7)	Yb1−N1	2.552(14)
		Eu1−N5	2.566(7)	Yb1−N2	2.512(13)
		Eu1−N6	2.580(7)	Yb1−N3	2.540(16)
		C22−C23	1.219(13)	C22−C23	1.26(3)
		C45−C46	1.182(13)	C45−C46	1.21(3)
Pt−C2−C3	173.7(4)	Pt−C23−C22	174.4(11)	Pt−C23−C22	175(2)
		Pt−C46−C45	177.7(10)	Pt−C46−C45	176(2)
C2−C3−C4	178.5(6)	C23−C22−C19	176.6(17)	C23−C22−C19	174(3)
C2−Pt−P1	89.46(13)	C23−Pt−P1	88.4(3)	C23−Pt−P1	90.0(6)
C2a−Pt−P1	176.04(13)	C46−Pt−P1	175.1(3)	C46−Pt−P1	177.8(8)
		C23−Pt−P2	177.2(3)	C23−Pt−P2	176.4(6)
		C46−Pt−P2	90.2(3)	C46−Pt−P2	87.8(6)
P1−Pt−P1a	86.69(6)	P1−Pt−P2	92.51(9)	P1−Pt−P2	92.52(18)
C2−Pt−C2a	94.4(3)	C23−Pt−C46	88.7(4)	C23−Pt−C46	89.6(8)

naphthyl)[18] and [(^{t}Bu$_2$bpy)Pt(C≡CAr)$_2$]·CH_2Cl_2 ($d_{H\cdots C}$ = 2.81−2.85 Å; Ar = 4-pyridyl).[19] The C2···H04B−C02B and C3···H04B−C02B angles are 126.4 and 136.6°, respectively, similar to those (129 and 143°) in [(tBu$_2$bpy)Pt(C≡CAr)$_2$]·CH_2Cl_2 (Ar = 4-pyridyl).[19] Consequently, substantial C−H···π(C≡C) interactions are likely operative between the solvate dichloromethane molecule and Pt(C≡CPhtpy)$_2$. Additionally, there also exists a C−H···N hydrogen-bonding interaction between the N3 atom in tpy and another solvate dichloromethane molecule ($d_{H\cdots N}$ = 2.736 Å, $d_{C01D\cdots N3}$ = 3.656 Å, ∠C01D−H3D···N3 = 158.67°) (D: 1.5 − x, −0.5 + y, 0.5 − z), similar to that observed in [(^{t}Bu$_2$bpy)Pt(C≡CAr)$_2$]·CH_2Cl_2 (Ar = 4-pyridyl).[19] As shown in Figure 2, one $\mathbf{1}\cdot 3CH_2Cl_2$ molecule links two neighboring ones at both sides in head-to-end form through C−H···π stacking interactions between the phenyl rings of dppe ($d_{C32\cdots X1F}$ = 3.617 Å; X1F denotes the centroid of the phenyl ring containing C25F−C30F) (F: 1.5 − x, 0.5 − y, 1.0 − z), respectively, leading to a 1-D chain structure.[20]

$\mathbf{6}\cdot{}^1/_2CH_2Cl_2\cdot{}^5/_2H_2O$ and $\mathbf{8}\cdot{}^1/_2CH_2Cl_2\cdot{}^1/_2H_2O$ crystallize in the triclinic system with space group $P\bar{1}$. The Eu^{III} or Yb^{III} ions are nine-coordinated with N_3O_6 donors to afford a distorted capped square antiprism. The Pt−P, Pt−C, and C≡C distances in $\mathbf{6}\cdot{}^1/_2CH_2Cl_2\cdot{}^5/_2H_2O$ and $\mathbf{8}\cdot{}^1/_2CH_2Cl_2\cdot{}^1/_2H_2O$ are comparable to those in $\mathbf{1}\cdot 3CH_2Cl_2$. The average Eu−N and Eu−O distances in $\mathbf{6}\cdot{}^1/_2CH_2Cl_2\cdot{}^5/_2H_2O$ are 2.57 and 2.43 Å, respectively. The former is obviously shorter than the Eu−N distances (2.645 and 2.663 Å) in the nine-coordinated terpyridine Eu^{III} species [Eu(DPM)$_3$terpy] (DPM = tris(dipivaloylmethanato), terpy = 2,2′:6′,2″-terpyridine),[21] while the latter is slightly longer than those reported in the literature.[22] For $\mathbf{8}\cdot{}^1/_2CH_2Cl_2\cdot{}^1/_2H_2O$, the average Yb−N distance (2.53 Å) is much longer than that (2.41 Å) in [Yb(NO$_3$)$_3$(L^1)] (L^1 = 2,2′:6′,2″-terpyridine).[23] The average Yb−O distance is 2.32 Å, much longer than that (average 2.258 Å) in eight-coordinated [Re(CO)$_3$Cl(μ-bpym)-Yb(fod)$_3$] (bpym = 2,2′-bipyrimidine, fod = tBuC(O)CH_2C(O)CF_2-CF_2CF_3).[2f] The Pt···Eu1 and Pt···Eu2 distances in $\mathbf{6}\cdot{}^1/_2CH_2Cl_2\cdot{}^5/_2H_2O$ are 14.35 and 14.23 Å, and the Pt···Yb1 and Pt···Yb2 separations in $\mathbf{8}\cdot{}^1/_2CH_2Cl_2\cdot{}^1/_2H_2O$ are 14.46 and 14.35 Å, respectively. The dihedral angles formed by the phenyl ring in C≡CPhtpy and the middle pyridyl ring of the terpyridyl moiety are 18.7 and 14.4° for $\mathbf{6}\cdot{}^1/_2CH_2Cl_2\cdot{}^5/_2H_2O$ and 14.8 and 13.5° for $\mathbf{8}\cdot{}^1/_2CH_2Cl_2\cdot{}^1/_2H_2O$, obviously reduced in comparison with those in $\mathbf{1}\cdot 3CH_2Cl_2$(32.8°), thus suggesting a better coplanar conformation for the C≡CPhtpy ligand upon formation of $PtLn_2$ arrays.

Table 3. UV−vis Absorption Spectral Data of 1−8

compd	λ_{em}/nm (ϵ/M^{-1} cm^{-1})
1	232 (79 040), 255 (53 450), 289 (58 390), 328 (61 630)
2	234 (84 400), 288 (87 950), 306 (92 840), 367 (64 420)
3	234 (86 920), 288 (86 830), 306 (98 550), 367 (63 330)
4	232 (72 520), 288 (74 780), 305 (75 630), 364 (51 530)
5	233 (78 180), 254 (54 920), 287 (57 030), 329 (56 300)
6	233 (75 100), 288 (78 820), 306 (84 180), 369 (56 170)
7	229 (81 080), 288 (72 470), 306 (84 550), 368 (51 310)
8	231 (77 340), 289 (100 700), 303 (99 270), 367 (43 860)

Absorption Spectra. UV−vis absorption spectral data of **1**−**8** in dichloromethane solutions at 298 K are summarized in Table 3. The absorption spectra are depicted in Figure 4 for **1**−**4** and Figure S3 (Supporting Information) for **5**−**8**. By comparison with the absorption features in free HC≡CPhtpy as well as with reference to the previous spectroscopic studies on related Pt^{II}−dppe[5a] and Pt^{II}−terpyridine complexes[24] and Pt^{II} complexes with oligopyridine-functionalized alkynyls,[11] high-energy bands at 230−260 nm and the absorptions at 280−330 nm in **1** and **5** are tentatively ascribed to dppe- or dppp-centered

(18) Müller, T. E.; Mingos, D. M. P.; Williams, D. J. *J. Chem. Soc., Chem. Commun*. **1994**, 1787.

(19) Lu, W.; Chan, M. C. W.; Zhu, N.; Che, C. M.; He, Z.; Wong, K. Y. *Chem. Eur. J.* **2003**, *9*, 6155.

(20) (a) Zheng, S. L.; Tong, M. L.; Fu, R. W.; Chen, X. M.; Ng, S. W. *Inorg. Chem*. **2001**, *40*, 3562. (b) Steiner, T.; Tamm, M.; Lutz, B.; Van der Mass, J. *J. Chem. Soc., Chem. Commun.* **1996**, 1127. (c) Tong, M. L.; Zheng, S. L.; Chen, X. M. *Polyhedron* **2000**, *19*, 1809.

(21) Holz, R. C.; Thompson, L. C. *Inorg. Chem*. **1988**, *27*, 4640.

(22) Yang, W. Y.; Chen, L.; Wang, S. *Inorg. Chem*. **2001**, *40*, 507.

(23) Drew, M. G. B.; Iveson, P. B.; Hudson, M. J.; Liljenzin, J. O.; Spjuth, L.; Cordier, P. Y.; Enarsson, Å.; Hill, C.; Madic, C. *Dalton Trans.* **2000**, 821.

(24) (a) Wadas, T. J.; Wang, Q. M.; Kim, Y. J.; Flaschenreim, C.; Blanton, T. N.; Eisenberg, R. *J. Am. Chem. Soc.* **2004**, *126*, 16841. (b) Yam, V. W. W.; Wong, K. M. C.; Zhu, N. *J. Am. Chem. Soc.* **2002**, *124*, 6506.

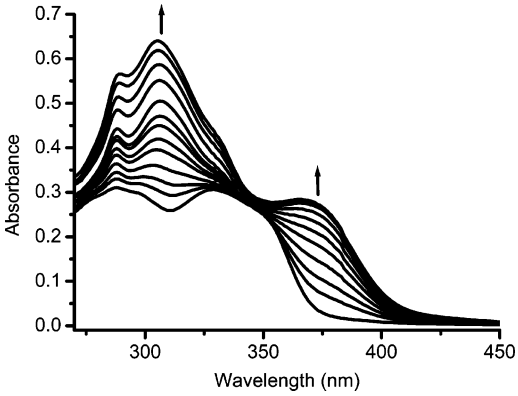

Figure 5. Changes in the UV−vis absorption spectra by titration of **1** with $Nd(hfac)_3(H_2O)_2$ in dichloromethane.

transitions and $\pi \rightarrow \pi^*$ transitions of C≡CPhtpy, respectively. The $\pi \rightarrow \pi^*$ absorption bands of C≡CPhtpy display slight red shifts relative to those in free HC≡CPhtpy, suggesting that the Pt^{II} center promotes delocalization of the C≡CPhtpy-based π and π^* orbitals involved in the optical transitions.[3a] Such a delocalization is consistent with the results of molecular orbital calculations on square-planar bis(acetylide) complexes of d^8 metals,[25] which implies that mixing of the metal-centered $d\pi$ orbitals with the π and π^* MOs of the acetylide ligands induces π-type conjugation through the metal center. Furthermore, **1** and **5** exhibit an additional lower energy shoulder absorption at ca. 345 nm, tailing to 450 nm ($\epsilon = 10^4-10^3$ M^{-1} cm^{-1}), ascribed tentatively to metal-perturbed $\pi \rightarrow \pi^*$ transitions in C≡CPhtpy mixed probably with some d(Pt) $\rightarrow \pi^*$(C≡CPhtpy) MLCT (metal-to-ligand charge transfer) character.[26,27]

In comparison with the absorption features of **1** or **5**, the remarkable difference in the absorption spectra of $PtLn_2$ complexes is the occurrence of a new band at 306 and an obvious red shift (ca. 20 nm) of the low-energy absorption. The former originates from the hfac ligand,[1c,2a] whereas the latter is caused by the enhanced d(Pt) $\rightarrow \pi^*$(C≡CPhtpy) MLCT transitions upon formation of the $PtLn_2$ heterotrinuclear arrays.[3,28] Addition of $Ln(hfac)_3(H_2O)_2$ to a dichloromethane solution of **1** or **5** results gradually in a deepening of the color from pale yellow to yellow, which is associated with the enhanced absorption of the MLCT transition in the visible region upon formation of $PtLn_2$ arrays. Figure 5 shows the changes of absorbance during the titration of **1** with $Nd(hfac)_3(H_2O)_2$ in the dichloromethane solution. Figure S4 (Supporting Information) shows the changes of absorbance at 367 nm in this titration versus the ratio of Nd^{III} to Pt^{II}, giving smooth curves that fits well to a 2:1 binding ratio between the Nd and Pt moieties. Assuming that $PtLn_2$ heterotrinuclear complexes are the main forms of the products in the solutions, the association constants for binding of $Ln(hfac)_3$ to **1** could be determined according to the titration results, and the values obtained are 4.80×10^{10}, 9.33×10^{10}, and 2.52×10^{11} for **2**−**4**, respectively. These constants are significantly larger than that of the 2,2′-bipyridyl-containing Pt_2Eu_2 species,[1c] due to the chelating ability of terpyridine being stronger than that of bipyridine.

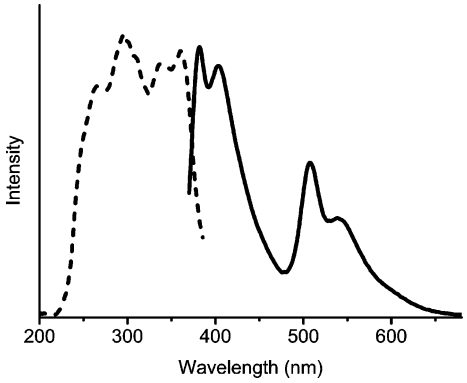

Figure 6. Excitation (dashed line) and emission (solid line) spectra of **1** in degassed dichloromethane.

Table 4. Luminescence Data for 1−8 at 298 K

	λ_{em}/nm (τ_{em}/μs)		
compd	solid	CH_2Cl_2 soln	Φ (%)[a,b]
1	403 (<0.20 ns)	382 sh, 404 (<0.2 ns)	2.21[b]
	518 sh, 554 (8.40 (76%), 1.16 (24%))	507 (3.71), 541 sh	1.24[b]
2	616 (306.4)	431 (<0.2 ns)	4.45[b]
		616 (984.3)	
3	1063 (weak)	452 (<0.20 ns)	
		1065 (weak)	
4	981 (13.6)	456 (<0.20 ns)	
		981 (15.5)	0.78[a]
5	403 (<0.20 ns)	384 sh, 404 (0.82 ns)	0.83[b]
	519 sh, 558 (10.43 (77%), 1.41 (23%))	508 (1.94), 542 sh	0.34[b]
6	615 (393.2)	428 (<0.2 ns)	
		616 (1095.6)	4.17[b]
7	1064.6 (weak)	436 (<0.2 ns)	
		1064 (weak)	
8		440 (<0.2 ns)	
	980 (14.64)	981 (14.62)	0.73[a]

[a] The quantum yields of Yb^{III} complexes in dichloromethane are estimated by the equation $\Phi = \tau_{obs}/\tau_0$, in which τ_{obs} is the observed emission lifetime and τ_0 is the radiative or "natural" lifetime within 2 ms. [b] The quantum yields of **1**, **2**, **5**, and **6** in degassed CH_2Cl_2 are determined relative to that of $[Ru(bpy)_3](PF_6)_2$ ($\Phi = 0.062$) in degassed CH_3CN.[10]

Luminescence. Excitation and emission spectra of **1** in degassed dichloromethane are illustrated in Figure 6, and those of **5** are depicted in Figure S5 (Supporting Information). The emission spectra of **1** and **5** in the solid state are depicted in Figure S6 (Supporting Information). Luminescence data and emission lifetimes are summarized in Table 4. Both **1** and **5** exhibit a short-lived emission ($\tau < 1$ ns) at ca. 400 nm and a long-lived emission at ca. 505−560 nm in both the solid state and degassed dichloromethane with lifetimes on the microsecond scale. The vibronic progression spacing of the high-energy bands is 1426 cm^{-1} for **1** and 1289 cm^{-1} for **5**, while that of the low-energy emission is 1240 cm^{-1} for **1** and 1235 cm^{-1} for **5** in degassed dichloromethane, which is typical of the ν(C=C) and ν(C=N) aromatic vibrational modes for the terpyridine ligands.[27b] The Stokes shift of the low-energy emission (8054 cm^{-1}) is much larger than that of the high-energy emission (1600 cm^{-1}) for **1** in degassed dichloromethane. The short lifetime, small Stokes shift, and similarity of emission energy with that in the free HC≡Cphtpy indicate distinctly that the high-energy, short-lived emission at ca. 400 nm is the ILCT (intraligand charger transfer) fluorescence of C≡Cphtpy from the $^1\pi \rightarrow \pi^*$ excited state.[3a,29] In contrast, the long lifetime and large Stokes shift of the low-energy emission at ca. 505−560 nm is suggestive of a

(25) Beljonne, D.; Wittmann, H. F.; Köhler, A.; Graham, S.; Younus, M.; Lewis, J.; Raithby, P. R.; Khan, M. S.; Friend, R. H.; Brédas, J. L. *J. Chem. Phys.* **1996**, *105*, 3868.

(26) Chakraborty, S.; Wadas, T. J.; Hester, H.; Flaschenreim, C.; Schmehl, R.; Eisenberg, R. *Inorg. Chem.* **2005**, *44*, 6284.

(27) (a) Wong, K. M. C.; Tang, W. S.; Lu, X. X.; Zhu, N.; Yam, V. W. W. *Inorg. Chem.* **2005**, *44*, 1492. (b) Yam, V. W. W.; Tang, R. P. L.; Wong, K. M. C.; Cheung, K. K. *Organometallics* **2001**, *20*, 4476.

(28) Ziessel, R.; Hissler, M.; El-ghayoury, A.; Harriman, A. *Coord. Chem. Rev.* **1998**, *178*−*180*, 1251.

(29) Waldeck, D. H. *Chem. Rev.* **1991**, *91*, 415.

triplet state parentage.[5b] It has been demonstrated that the phosphorescence emission of Pt^{II}−phosphine−alkynyl complexes frequently originates from the metal-perturbed $^3\pi \rightarrow \pi^*$-(C≡C) excited state of the alkynyl ligand with an extended chromophore due to the strong spin−orbit coupling induced by the heavy Pt^{II} center.[3a,5a,b] The room-temperature phosphorescence of **1** and **5** is thus ascribed to the extended and conjugated chromophore of Phtpy as well as the strong spin−orbital coupling induced by the Pt^{II} coordination, probably involving some ^{3}MLCT character.[20,25,27b,30] As a consequence, the phosphorescence emissions in both **1** and **5** arise probably from an admixture of ^{3}MLCT (d(Pt) → π^*(C≡CPhtpy)) and intraligand ^{3}ILCT ($\pi \rightarrow \pi^*$(C≡CPhtpy)) triplet excited states.[31] This assignment is supported by theoretical studies on the related mononuclear complexes *trans*-$Pt(PEt_3)_2(C{\equiv}CPh)_2$ and *trans*-$Pt(PEt_3)_2(C{\equiv}CC_6H_4C{\equiv}CH)_2$[32] and model compounds *cis*-Pt(dHpe)$(C{\equiv}CC{\equiv}CH)_2$ and *cis*-Pt(dHpp)$(C{\equiv}CC{\equiv}CH)_2$ (the hydrogen-substituted models of *cis*-Pt(dppe)$(C{\equiv}CC{\equiv}CH)_2$ and *cis*-Pt(dppp)$(C{\equiv}CC{\equiv}CH)_2$).[14a] The calculated results show that the highest occupied molecular orbitals (HOMO) are the mixing of d(Pt) orbitals and π orbitals of the alkynyl ligand, while the lowest unoccupied molecular orbitals (LUMO) only contain π^* orbitals of the alkynyl ligand, in good accord with the emission assignment from a mixed ^{3}ILCT ($\pi \rightarrow \pi^*$(C≡CR))/^{3}MLCT (dπ(Pt) → π^*(C≡CR)) transition.[32] Although second- and third-row transition-metal complexes frequently exhibit room-temperature phosphorescence resulting from the strong spin−orbit coupling induced by heavy-atom effects,[33] room-temperature phosphorescence occurs mostly in the oligomers, polymers, and copolymers for Pt^{II}−acetylide−phosphine systems.[5c−e,34,35] Few mononuclear Pt^{II} species are phosphorescent at room temperature, though numerous mononuclear Pt(II)−acetylide−phosphine complexes have been synthesized.[12,13a,36] To the best of our knowledge, only very limited examples such as *cis*-Pt(dppe)-$(C{\equiv}CR)_2$ (R = C_6H_4-*p*-NO_2),[5a] *cis*-Pt(dppe)$(C{\equiv}C$-nap$)_2$ (C≡C-nap = 1-ethynylnaphthalene), and platinum(II)-containing phenyl−ethynyl oligomers[37] show room-temperature phosphorescence from $^3\pi \rightarrow \pi^*$ states of the corresponding alkynyl ligands predominantly. The similar complexes Pt(dppe)$(4\text{-ES})_2$ and $Pt(PBu_3)(4\text{-ES})_2$ (4-ES = 4-ethynylstilbene) exhibit phosphorescence from the$^3\pi \rightarrow \pi^*$ state of 4-ES only at low temperature below 140 K in rigid glasses.[3a]

The luminescence data of the $PtLn_2$ heterotrinuclear species **2**−**4** and **6**−**8** are also summarized in Table 4. Upon excitation at λ_{ex} = 250−450 nm, the $PtLn_2$ complexes show characteristic

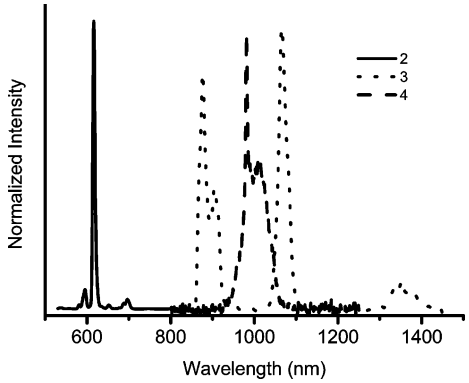

Figure 7. Ln^{III} emission spectra of **2** (solid line), **3** (dotted line), and **4** (dashed line) in degassed dichloromethane solution.

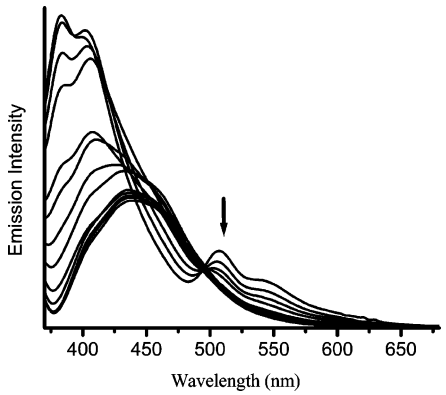

Figure 8. Luminescence titration of **1** with $Nd(hfac)_3(H_2O)_2$ in dichloromethane.

emissions of the corresponding Ln^{III} ions with microsecond to millisecond (for Eu^{III} species) ranges of lifetimes in both the solid state and dichloromethane. The observation of characteristic emissions from the corresponding Ln^{III} centers by excitation of Pt-based absorption (λ_{ex} = 350−450 nm) demonstrated unambiguously that the sensitized lanthanide luminescence is indeed achieved by $Pt^{II} \rightarrow Ln^{III}$ energy transfer from the Pt-based antenna triple states, because $Ln(hfac)_3(H_2O)_2$ species have no obvious absorption in this region. The characteristic Ln^{III} emission spectra in dichloromethane solutions are illustrated in Figure 7 for **2**−**4** and Figure S7 (Supporting Information) for **6**−**8**. As expected, five emission bands were observed for Eu species at 581 ($^5D_0 \rightarrow {}^7F_0$), 596 ($^5D_0 \rightarrow {}^7F_1$), 616 ($^5D_0 \rightarrow {}^7F_2$), 652 ($^5D_0 \rightarrow {}^7F_3$), and 687 nm ($^5D_0 \rightarrow {}^7F_4$), three for Nd species at 877 ($^4F_{3/2} \rightarrow {}^4I_{9/2}$), 1066 ($^4F_{3/2} \rightarrow {}^4I_{11/2}$), and 1339 nm ($^4F_{3/2} \rightarrow {}^4I_{13/2}$), and one for Yb species at 981 nm ($^2F_{5/2} \rightarrow {}^2F_{7/2}$). In dichloromethane solutions of the $PtLn_2$ complexes, ILCT fluorescence from the $^1\pi \rightarrow \pi^*$ excited state of C≡Cphtpy is observed with a maximum at 420−460 nm, whereas low-energy phosphorescence emission from ^{3}ILCT ($\pi \rightarrow \pi^*$(C≡CPhtpy))/^{3}MLCT (dπ(Pt) → π^*(C≡CPhtpy)) triplet states is quenched. Since the tail of the ILCT fluorescence emission may overlap with the phosphorescence region of the $Pt(C{\equiv}Cphtpy)_2$ moiety, it is uncertain whether the phosphorescence of the Pt^{II} alkynyl chromophore is entirely quenched.

Emission titrations have been carried out in aerated dichloromethane solutions. Figure 8 displays the changes during titration of **1** using $Nd(hfac)_3(H_2O)_2$ with an excitation wavelength at 355 nm. While the low-energy phosphorescence is reduced remarkably with gradual addition of $Nd(hfac)_3(H_2O)_2$,

(30) (a) Büchner, R.; Field, J. S.; Haines, R. J. *Inorg. Chem.* **1997**, *36*, 3952. (b) Büchner, R.; Cunningham, C. T.; Field, J. S.; Haines, R. J.; McMillin, D. R.; Summerton, G. C. *J. Chem. Soc., Dalton Trans.* **1999**, 711.

(31) (a) Görner, H. *J. Phys. Chem.* **1989**, *93*, 1826. (b) Wong, K. M. C.; Tang, W. S.; Chu, B. W. K.; Zhu, N.; Yam, V. W. W. *Organometallics* **2004**, *23*, 3459.

(32) (a) Emmert, L. A.; Choi, W.; Marshall, J. A.; Yang, J.; Meyer, L. A.; Brozik, J. A. *J. Phys. Chem. A* **2003**, *107*, 11340.

(33) Evans, R. C.; Douglas, P.; Winscom, C. J. *Coord. Chem. Rev.* **2006**, *250*, 2093.

(34) (a) Wittmann, H. F.; Friend, R. H.; Khan, M. S.; Lewis, J. *J. Chem. Phys.* **1994**, *101*, 2693. (b) Wilson, J. S.; Köhler, A.; Friend, R. H.; Al-Suti, M. K.; Al-Mandhary, M. R. A.; Khan, M. S.; Raithby, P. R. *J. Chem. Phys.* **2000**, *113*, 7627.

(35) Roundhill, D. M.; Gray, H. B.; Che, C. M. *Acc. Chem. Res.* **1989**, *22*, 55.

(36) (a) ALQaisi, S. M.; Galat, K. J.; Chai, M.; Ray, D. G., III; Rinaldi, P. L.; Tessier, C. A.; Youngs, W. *J. Am. Chem. Soc.* **1998**, *120*, 12149. (b) Campbell K.; Johnson, C. A., II; McDonald, R.; Ferguson, M. J.; Haley, M. M.; Tykwinski, R. R. *Angew. Chem., Int. Ed.* **2004**, *43*, 5967.

(37) (a) Pomestchenko, I. E.; Castellano, F. N. *J. Phys. Chem. A* **2004**, *108*, 3485. (b) Rogers, J. E.; Cooper, T. M.; Fleitz, P. A.; Glass, D. J.; McLean, D. G. *J. Phys. Chem. A* **2002**, *106*, 10108.

the high-energy fluorescence is obviously red-shifted relative to the precursor **1** with a maximum from 404 to 433 nm, arising probably from the increasing rigidity and the more extended conjugacy of the C≡CPhtpy upon incorporation of **1** with Nd(hfac)$_3$ units. Titrations of **1** and **5** with other Ln(hfac)$_3$(H$_2$O)$_2$ species also show similar behavior. It has been demonstrated that, once they are bonded to a metal ion such as Zn^{II} or protonated at the nitrogen atoms,[38] the terpyridyl ligands often display red-shifted fluorescence emission as observed herein. Except for energy transfer to Ln^{III} centers, rapid quenching of the phosphorescence in the Pt^{II} alkynyl chromophore is probably relevant to the additional vibrational pathways brought by combination of Ln(hfac)$_3$ for deactivation of the excited state and the perturbation of the triplet level because of the presence of a 3+ charge.[2f] In addition, oxygen may be another important factor, since the luminescence titration was carried out in aerated dichloromethane solutions.

As for Pt → Ln energy transfer pathways in the PtLn$_2$ species, both the Dexter and Förster mechanisms are possibly operative because of the conjugated character of the Phtpy ligands, the favorable spectral overlapping between Pt-based emission and the f−f absorptions in the relevant region,[2f] and the moderate Pt−Ln distance (ca. 14.2 Å) across the bridging C≡Cphtpy ligand. In the PtLn$_2$ species with Ln = Eu^{III}, Nd^{III}, there exist the transitions that follow the selection rules for both the Dexter ($|\Delta J| = 0, 1$) (with the exception of $J = J' = 0$, which is forbidden) and Förster types ($|\Delta J| = 2, 4, 6$).[2f] For the PtYb$_2$ species, since there only exists one possible transition ($^2F_{7/2} \rightarrow {}^2F_{5/2}$) for Yb^{III} ions, a Dexter-type energy transfer is favored.[2a,f]

(38) (a) Goodall, W.; Wild, K.; Arm, K. J.; Williams, J. A. G. *J. Chem. Soc., Perkin Trans. 2* **2002**, 1669. (b) Alcock, N. W.; Barker, P. R.; Haider, J. M.; Hannon, M. J.; Painting, C. L.; Pikramenou, Z.; Plummer, E. A.; Rissanen K.; Saarenketo, P. *Dalton Trans.* **2000**, 1447.

Summary

cis-Pt(dppe)(C≡CPhtpy)$_2$ and *cis*-Pt(dppp)(C≡CPhtpy)$_2$ exhibit strong dual room-temperature emissions including short-lived fluorescence and long-lived phosphorescence. The low-energy emission originates likely from an admixture of ^{3}ILCT ($\pi \rightarrow \pi^*$(C≡Cphtpy)) and ^{3}MLCT (d(Pt) → π^*(C≡Cphtpy)) triplet states due to the extended π-conjugated chromophore and the strong spin−orbital coupling induced by the Pt^{II} center. The lower energy absorption and strong room-temperature phosphorescence qualify hte precursors **1** and **5** as good energy donors to facilitate Pt → Ln energy transfer in the corresponding heterotrinuclear adducts with Ln(hfac)$_3$. All of the PtLn$_2$ complexes exhibit characteristic Ln^{III} emissions sensitized by ^{3}ILCT and ^{3}MLCT excited triplet states through efficient energy transfer from the Pt^{II} alkynyl based antenna chromophore.

Acknowledgment. This work was supported financially by the NSFC (Grant Nos. 90401005, 20490210, 20521101, and 20625101), the NSF of Fujian Province (Grant No. E0420002), the 973 project (Grant No. 2007CB815304) from MSTC and the Key Project from CAS (Grant No. KJCX2-YW-H01).

Supporting Information Available: Figures giving additional spectroscopic and structural characterization data and emission spectra of the compounds prepared and CIF files giving X-ray crystallographic files for **1**·3CH$_2$Cl$_2$, **6**·$^1/_2$CH$_2$Cl$_2$·$^5/_2$H$_2$O, and **8**·$^1/_2$CH$_2$Cl$_2$·$^1/_2$H$_2$O. This material is available free of charge via the Internet at http://pubs.acs.org.

OM070130H